Rafidain Journal of Science
https://rsci.mosuljournals.com

Vol. 33, No. 4, pp. 137-147, 2024

The Effect of Green Synthesis ZnO NPs on Sun Protection Factor of Sunblock Lotion

Himdad H. Azeez
Physics Department/ College of Education/ Shaqlawa/ Salahaddin University-Erbil/ Iraq
Bestoon A. Gozeh
Department of Information Technology/ Shaqlawa Technical College/ Erbil Polytechnic University/ Iraq
Hero H. Azeez
Erbil Dermatology Teaching Center/ Iraq
Lary H. Slewa
Physics Department/ College of Science/ Salahaddin University-Erbil/ Iraq

p-ISSN: 1608-9391
e -ISSN: 2664-2786

Article information

Received: 6/5//2024
Revised: 28/6/2024
Accepted: 8/7/2024

DOI: 10.33899/rjs.2024.185392

corresponding author:
Mr. Himdad H. Azeez
himdad.azeez@su.edu.krd.
Dr. Bestoon A. Gozeh
bestoon.hamadameen@su.edu.krd.
Ms. Hero H. Azeez
dr.hearohammad@gmail.com.
Dr. Lary H. Slewa,
lary.slewa@su.edu.krd

ABSTRACT

In modern times, there's a significant focus on green synthesis, which involves the environmentally friendly production of nanoparticles without using harmful chemicals or toxic solvents. This approach, popular in biological methods, has gained considerable attention. Leveraging natural sources such as plants and microorganisms is a common method for green synthesis. Zinc oxide nanoparticles (ZnO NPs) rank as the second most prevalent among metal oxides, largely owing to their affordability, safety, and simple production process. A sustainable method was employed to create these nanoparticles, which entailed extracting them from the (Lepidium sativum L.) plant along with zinc acetate dihydrate. The ZnO NPs underwent thorough characterization techniques to analyze their structure, surface morphology, and optical and chemical properties. The ZnO nanoparticles exhibited an average crystalline size of 26.78 nm, with FE-SEM confirming an average agglomerated nanoparticle size of 64 nm. Subsequently, varying weight percentages of these nanoparticles were incorporated into Sunblock Lotion to investigate their impact on enhancing the sun protection factor (SPF) of the lotion. The results demonstrated a noticeable increase in SPF with the higher concentrations ZnO NPs.

Keywords: ZnO; SPF; XRD; EDX; Green approach.

INTRODUCTION

Nanotechnology means using or making the machines or systems on the nanoscale. At the nanoscale size, the machines or systems get more specifications than in the bulk size for example small in size, lightweight, and fast response specifications (Panahi *et al*., 2024). The nanoparticles mean the particles at the nanoscale size (1-100) nm. The nanoparticles have different shapes like spherical, hexagonal, conical, etc. (Xie *et al*., 2024). However, according to dimensions, the materials have zero dimension, for instance, quantum dot, one dimension for instance nano rod, two-dimensions like thin film, and also three dimensions like breaking bulk materials to get nano size particles (Vijayaram *et al*., 2024). Also, the zinc oxide has hexagonal wurtzite crystal structure, good conductivity, high electron mobility, strong and good transparency (Senthilkumar and Sivakumar, 2014). It is popular metal oxide nanoparticles because have more applications in many areas or industries like in agriculture, water purification, medical, fashion, cosmetics, etc. (Sabir *et al.,* 2014).

Now the researchers focus on the biological method for the preparation of nanoparticles because it is cheap, safe, and large production. The biological method or green method means using natural sources like (algae, fungus, plants, and bacteria) (Fakhari *et al.*, 2019). Between these natural sources, the plant usage is a trend by researchers nowadays because it has more phytochemicals like polyphenols, sugar, flavonoids, and ascorbic acid (Vitamin C) that are phytochemicals needed for cupping and stabilizing nanoparticles (Agarwal *et al.,* 2017).

Because of the harmful, cosmic rays that incoming from outside of the atmosphere like Ultra-Violet radiation, there are many health problems concerning the skin are produced (Shchepkin *et al*., 2024). The wavelength from 320-400 nm is related to UVA, 290-320 related to UVB, and 200-290 is related to UVC. UVC is absorbed completely by the atmosphere. But UVB and UVA are not absorbed completely and may cause many skin problems (Mbanga *et al.*, 2014). UVB is the main source of sunburn erythema and skin cancer, due to pyrimidine dimers creation. UVA is concerned to photoaging, tanning and can indirectly damage DNA (Mesías *et al.*, 2017). So, the sun screen creams and lotions are suggested to avoid the penetration and irradiation of ultraviolet radiation (Pniewska and Kalinowska-Lis, 2024).

Chemical and physical sunscreens are two popular types of sunscreens. The UV ray absorbed and also changed to the heat in chemical sunscreens. Physical sunscreens make a shield on the skin and reflects the radiations (Kaur, 2023).

Because of good transparency and reflectivity, zinc oxide nanoparticles is used in sunblock product industry to avoid ultraviolet ray (Ann *et al.,* 2015). There are two methods to determine the SPF value these are *vivo* and *vitro* methods. To know the efficiency of sun cream, SPF have to be determined. Due to the expensive and long-time *in vivo* method, the *vitro* technique is applied to evaluate SPF value (Sudhahar, 2013). The wavelength range (290 to 320) nm in ultraviolet spectroscopy was used to absorbance measuring and equation of Mansur is used to calculate the SPF value (Dutra *et al.*, 2004). The ratio of ZnO NPs in sunblock lotion is subject of this study.

Garden cress (*Lepidium sativum* L.), an annual, upright, smooth herbaceous plant, is cultivated for culinary uses across various regions in Asia and Europe and belongs to the Brassicaceae family (Albalawi *et al.,* 2023). It contains numerous bioactive compounds, such as cardiac glycosides, alkaloids, phenolics, flavonoids, carbohydrates, proteins, amino acids, tannins, and uric acid (Ben Farhat *et al.,* 2024). Extensive pharmacological studies have shown that it possesses a wide range of medicinal properties, including antimicrobial, antidiabetic, antioxidant, anticancer, anti-inflammatory, and antipyretic effects (Al-Saran *et al.,* 2024). Therefore, in this study, *Lepidium sativum* L. was used as a cupping and stabilizing agent in the synthesis of zinc oxide nanoparticles due to its rich phytochemical content.

METHOD

In Erbil city, *Lepidium sativum* L. leaves were gathered, and subsequently sliced into small pieces. These parts were transformed into a paste using a mortar and pestle. Following this, 9 grams of the resulting paste were combined with d water (100 ml). The mixture underwent heating with stirring for approximately thirty minutes at 70°C. Afterward, the mixture was filtered through filter paper to obtain a clear solution. In a separate process, at 85°C, the plant extract (50 ml) with 2 grams of Zn $(CH_3COO)_2 \cdot 2H_2O$ were mixed. A paste was formed after the water evaporation of the mixture. Subsequently, this paste underwent calcination at 350°C to produce Zinc Oxide nanoparticles in powder form Fig. (1).

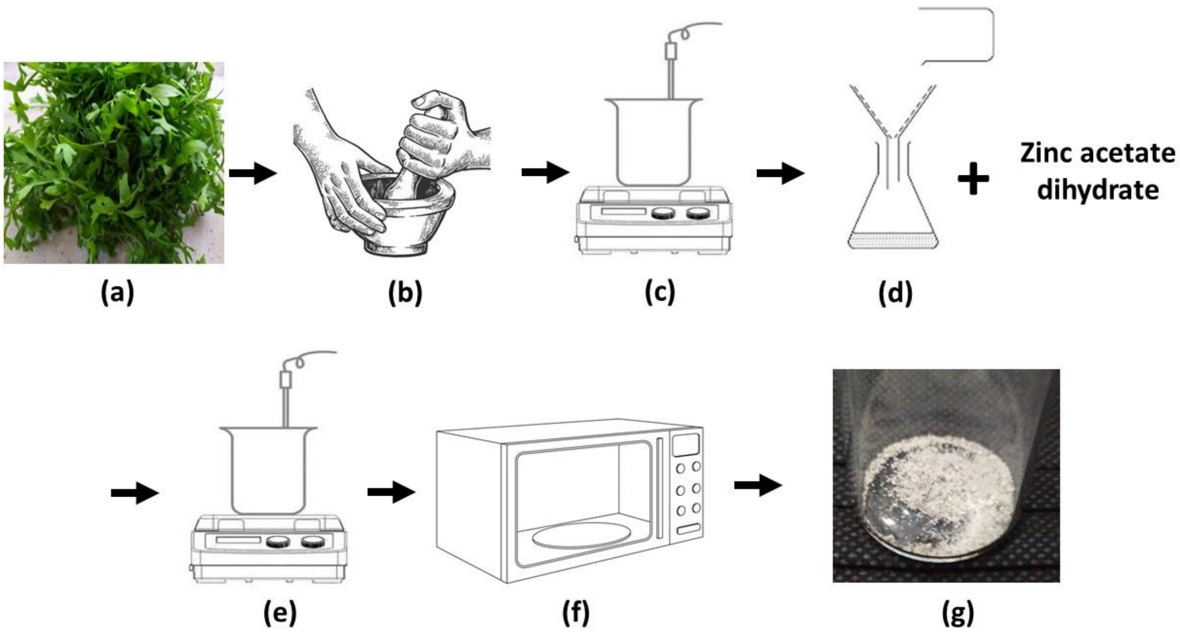

Fig. 1: Illustrates the process of producing zinc oxide nanoparticles (ZnO NPs) from Lepidium sativum L. leaves. (a) It involves washing the leaves, (b) Crushing them with a mortar and pestle, (c) Mixing the paste with distilled water and heating it at 70°C, (d) Filtering the product, combining it with zinc acetate dihydrate, (e) Heating and stirring until it forms a paste, (f) Burning the paste at 350°C, and (g) Finally obtaining the ZnO NPs powder.

ZnO NPs application in cosmetic

A commercial physical sun cream product, specifically Hydroderm sunblock lotion (Sun Protection Factor = 30) was chosen. Different specimens were formulated for comparison. the 1st specimen was Sunblock lotion without any ZnO NPs. 5.8wt% of ZnO NPs was present in the 2nd specimen, 11.1wt% of ZnO NPs was existence in the 3rd specimen. These specimens were analyzed through UV-Vis technique. Ultimately, Mansur's equation was employed to evaluate (SPF) value of the sunblock lotions.

$$\mathrm{SPF} = \mathrm{CF} \times \sum_{290}^{320} \mathrm{EE}(\lambda) \times \mathrm{I}(\lambda) \times \mathrm{Abs}(\lambda) \ldots\ldots\ldots\ldots\ldots\ldots (1)$$

In this context, the correction factor (CF) is specified as 10, with $\mathrm{Abs}(\lambda)$ representing absorbance, $\mathrm{EE}(\lambda)$ corresponding to the erythema effect spectrum, and $\mathrm{I}(\lambda)$ indicating the solar intensity spectrum. The absorbance spectra were multiplied by the corresponding $\mathrm{EE}(\lambda) \times \mathrm{I}(\lambda)$

constants in (Table 1). The resulting values were then summed $\sum_{290}^{320} \mathrm{EE}(\lambda) \times \mathrm{I}(\lambda) \times \mathrm{Abs}(\lambda)$ and subsequently multiplied by the correction factor (10).

Table 1: Standardized product function utilized in SPF calculation (Nkosi and Thembane, 2024).

λ nm	$\sum_{290}^{320} \mathbf{EE}(\boldsymbol{\lambda}) \times \mathbf{I}(\boldsymbol{\lambda})$
290	0.015
295	0.0817
300	0.2874
305	0.3278
310	0.1864
315	0.0839
320	0.018

RESULTS AND DISCUSSION

UV-Vi's spectra of the plant extract

In green synthesis the phytochemicals inside the plant extract act a reduction, capping, and stabilizing agent for the synthesis of zinc oxide nanoparticles (Ovais *et al.*, 2018). Before using the selected plant to synthesis zinc oxide nanoparticles, the plant must be characterized by a UV-Vis spectrometer as the quantitative measurement to know the existence of the chemical compositions inside the plant (Pirtarighat *et al.*, 2019). In UV-Vis spectra, the two peaks were showed, 1st peak at 263 nm and 2nd peak at 324 nm, they focus on phenolic substances, specifically flavonoids and similar aromatic organic compounds (Tariq *et al.*, 2023). So, the plant is suitable for synthesis ZnO NPs.

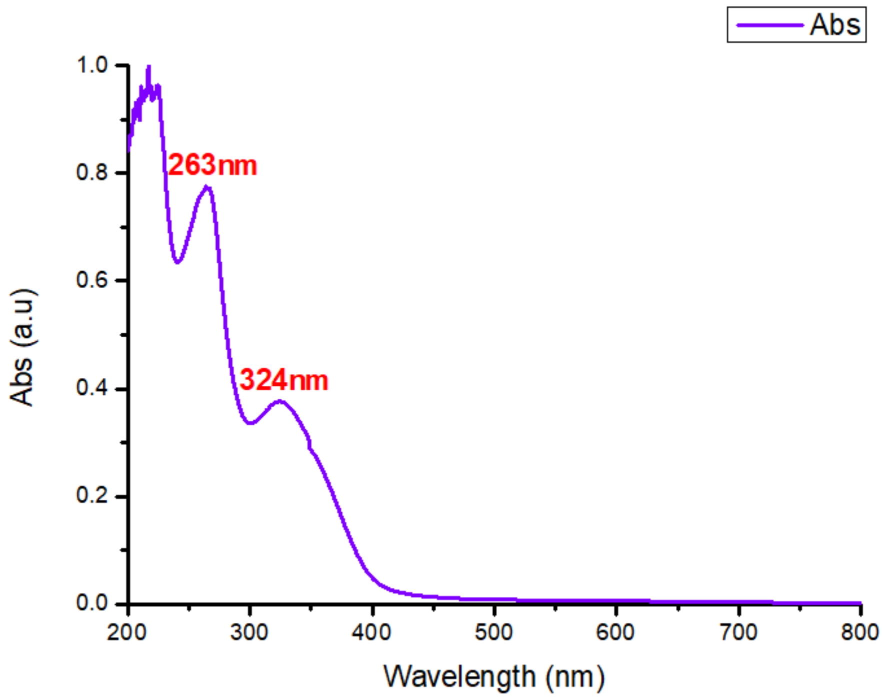

Fig. 2: UV Vis spectra of plant extract.

FT-IR characterization of the (*Lepidium sativum* L.) plant extract

FT-IR is the qualitative measurement to now the chemical compounds inside the plant.

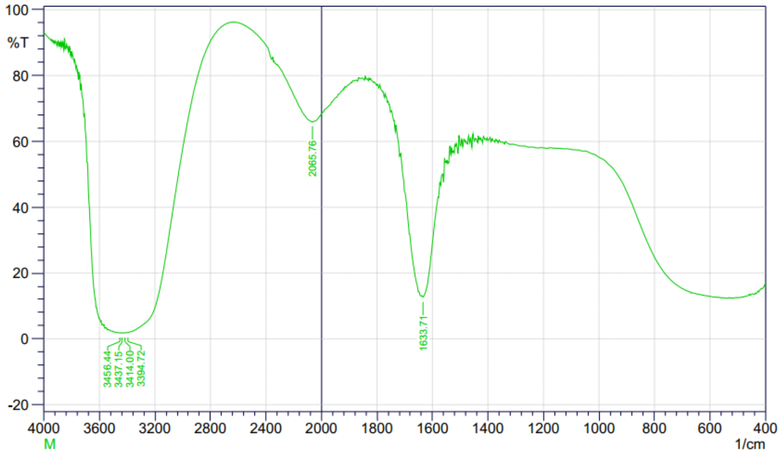

Fig. 3: FT-IR spectra of (*Lepidium sativum* L.) leave extract.

In Fig. (3), the peak detected at (1633 cm^{-1}) signifies the stretching vibration of the carbonyl group (C=O) within a conjugated arrangement, indicating the existence of either ketones or aldehydes (Mohamed *et al.*, 2017). Summit observed at (2065 cm^{-1}) related to the existence of triple bonds, particularly in alkynes. Stretching vibration of carbon-carbon triple bond (C≡C) is a common interpretation for this wavenumber. The range of (3394-3456 cm^{-1}) covers the extensive stretching vibrations of O-H bonds, suggesting the existence of hydroxyl groups. It is associated with alcohol or phenol functional groups, which are commonly found in organic compounds (Gipson *et al.*, 2015). So, *Lepidium sativum* is suitable for preparation of ZnO NPs.

ZnO NPs (UV-Vis spectrum)

UV-Vi's spectrum of the Zinc Oxide NPs revealed a single peak associated with surface plasmon resonance at 370 nm Fig. (4). This peak indicates high purity, monodispersity, and a smaller size compared to bulk zinc oxide. The observed blue-shifted peak aligns with the quantum confinement effect (Qin *et al.*, 2011; Varadavenkatesan *et al.*, 2019).

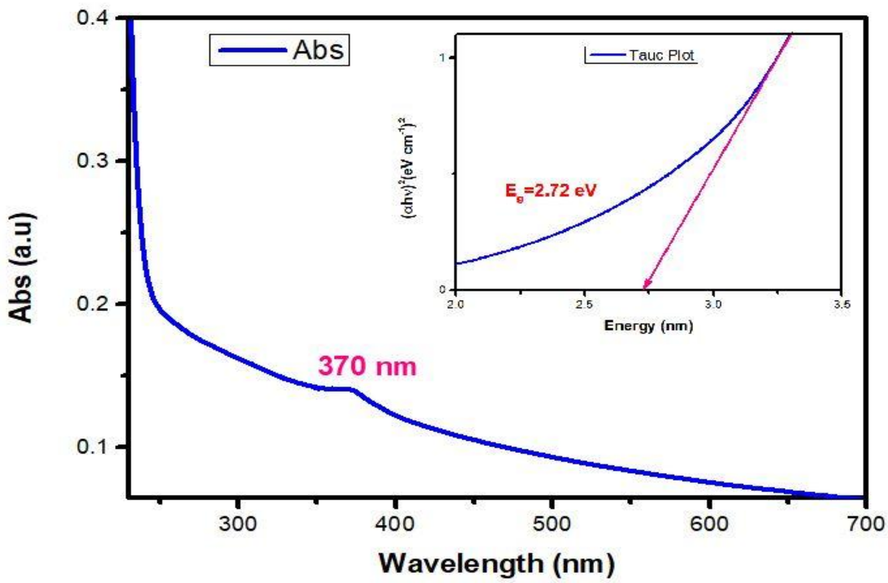

Fig. 4: ZnO NPs UV-Vis spectrum.

After that, energy bandgap of the sample determined by drawing the Tauc plot (Feng *et al.*, 2015).

$$\alpha h v = B(hv - E_g)^n \dots\dots\dots\dots\dots\dots\dots\dots\dots\dots\dots\dots\dots\dots\dots (2)$$

It was equal to (2.72) eV. So, the energy-gap is smaller than the bulk Zinc Oxide energy-gap that is normal in green synthesis. The antioxidants of the plant cover sample surface. So energy bandgap of the nanoparticles will be decreased (Khan *et al.*, 2019).

ZnO NPs (FT-IR spectrum)

In Fig. (5), the peak observed at 1132 cm^{-1} is assigned to the stretching vibration of C-O bonds, suggesting the existence of ether or alcoholic functional groups (Georgakopoulos, 2003; Oh *et al.*, 2005). The peak noted at 1435 cm^{-1} is linked to the bending vibration of CH_3 groups, indicating the presence of methyl groups within the sample (El-Hendawy, 2006). The peak observed at 1687 cm^{-1} indicates the stretching vibration of C=O bonds, suggesting the presence of carbonyl groups, similar to those found in ketones or aldehydes (Tan *et al.*, 2023). The peak detected at 3464 cm^{-1} corresponds to the stretching vibration of O-H bonds, suggesting the presence of hydroxyl groups, akin to those found in alcohols or phenols (Bhattacharyya *et al.*, 2024).

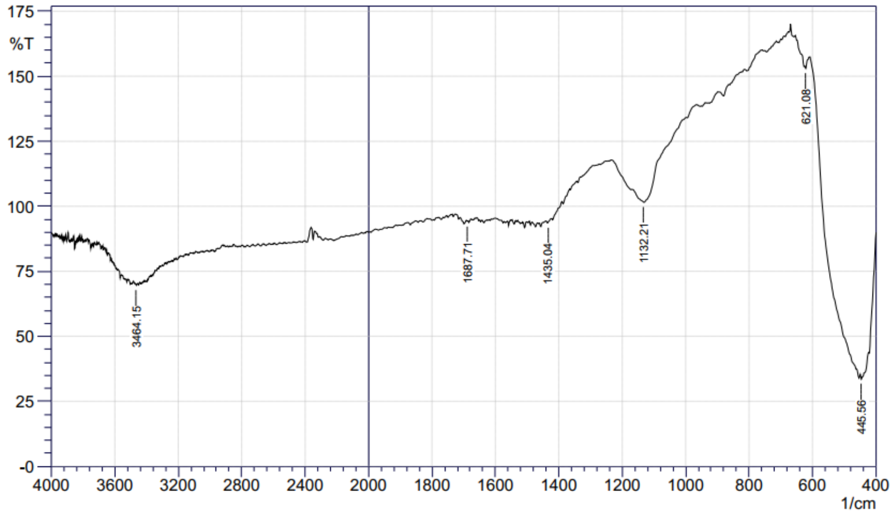

Fig. 5: FT IR analysis of sample.

XRD spectra of the sample.

Our sample was characterized by XRD technique to now the structure and crystalline size of the sample.

XRD spectra in Fig. (6) involved 11 peaks concerning the planes ((100), (002), (101), (102), (110), (103), (200), (112), (201), (004) and (202)) and acceptable with (JCPDS card No.89-0510) of Zinc Oxide (Thambidurai *et al.*, 2020).

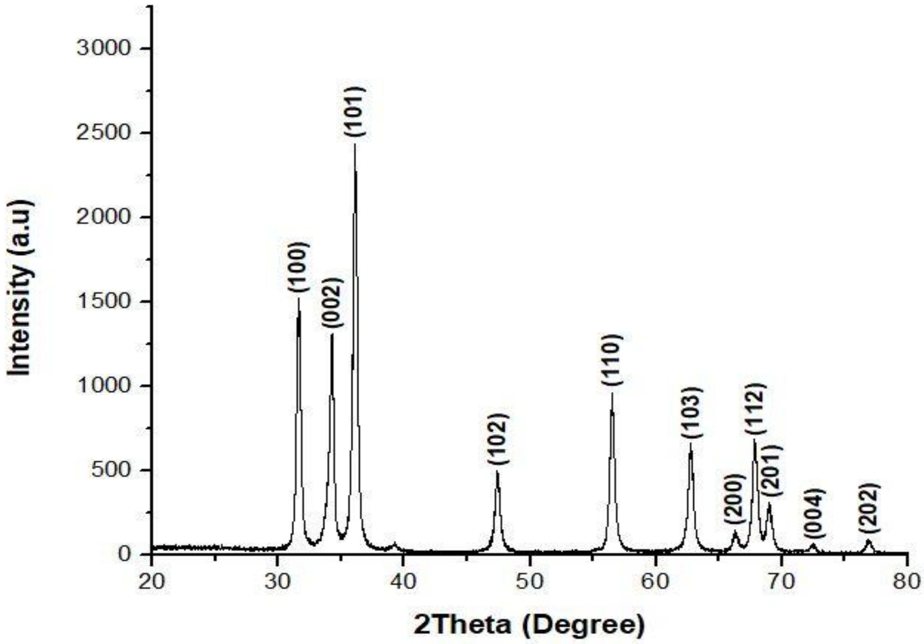

Fig. 6: XRD spectra of the sample.

The crystalline size of the sample, computed using Debye-Scherrer's equation, was found to be 26.78 nanometers.

$$D = \frac{k\lambda}{\beta \cos\theta} \dots\dots\dots\dots\dots\dots\dots\dots\dots\dots\dots\dots\dots\dots. \dots\dots (3)$$

Crystal size is denoted by D, X-Ray wavelength ($\lambda = 0.15406\, nm$), Shape factor is k= 0.9, β is symbol of full width at half maximum and θ is angle of diffraction (Vijayalakshmi and Rajendran, 2012).

FE-SEM image of the sample.

The sample was characterized using the FE-SEM technique to determine the size and shape of the ZnO NPs. The FE-SEM analysis showed that the particles are in the nanoscale, with a size of 64 nm and a spherical shape, as shown in Fig. (7).

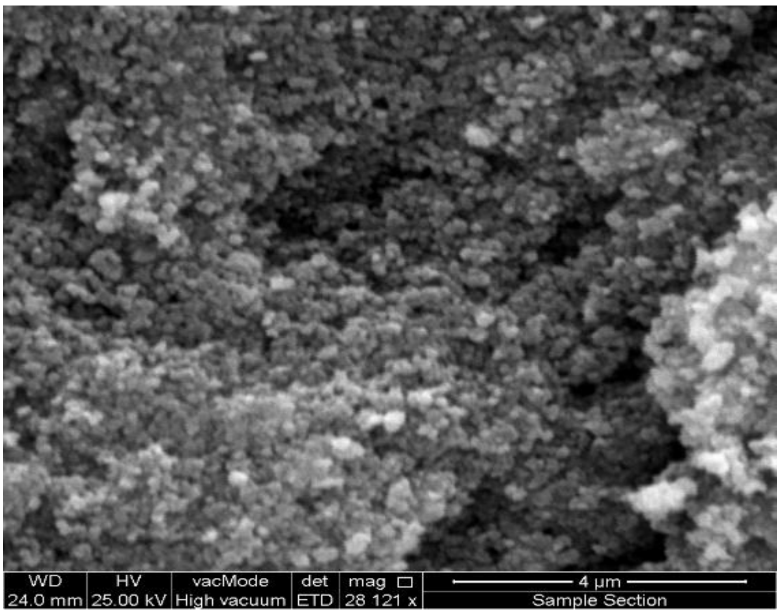

Fig. 7: FE-SEM image of sample.

SPF developing

UV-Vis spectroscopy was utilized to analyze all the samples to know the absorbance of in (UVA and UVB) regions Fig. (8) and also to calculate the sun protection factor (Table 2).

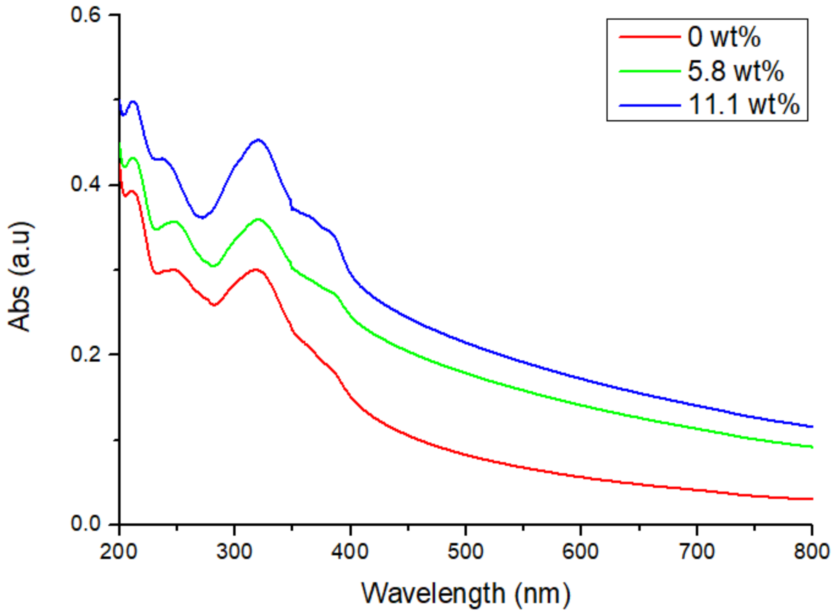

Fig. 8: UV-Vis spectra of the samples.

Table 2: Sun protection factor of the samples.

Name	ZnO NPs wt%	SPF
Sample 1	0	28.9
Sample 2	5.8	34.2
Sample 3	11.1	43

It is clear that all samples are active in both ranges the (UVB and UVA) regions.

The UV-Vis spectra in Fig. (8) and the SPF results of the samples in (Table 2) show that by increasing amount of ZnO NPs in the sunblock lotion, the absorbance peaks and the SPF values were increased. This has come back to high reflectivity and surface area of ZnO NPs. And SPF value that was put on the label is higher than the calculated SPF value over all the zinc oxide nanoparticles significantly influences the efficiency of sunblock lotion.

CONCLUSIONS

Lepidium sativum L. and zinc acetate dihydrate were used for creating of ZnO NPs. UV-Vis and FT-IR spectroscopy have confirmed the presence of active constituents within the plant extract, which effectively reduce, cap, and stabilize the nanoparticles. Following that, XRD characterization was conducted to ascertain the crystalline size, confirming the identity of the sample as ZnO NPs with a crystalline size measuring 26.78 nm. The FE-SEM analysis indicated agglomeration particle size was equal to 64 nm and spherical morphology.

The study involved the integration of Zinc Oxide nanoparticles into a physical sunblock lotion to augment its Sun Protection Factor (SPF), with varying concentrations. Characterization via UV-Vis Spectroscopy unveiled distinctions between the labelled and computed SPF values. As Zinc Oxide nanoparticle concentration rose, absorbance peaks in both UVB and UVA spectra intensified, leading to increased SPF values.

In essence, this research emphasizes the influence of environmentally friendly synthesized ZnO nanoparticles on the effectiveness of sunscreen blockers, even when present in minimal amounts.

ACKNOWLEDGMENT

We would like to extend our thanks to Salahaddin University-Erbil and the Soran Research Center for their valuable support in the characterization of samples during the course of our research.

REFERENCES

Agarwal, H.; Kumar, S.V.; Rajeshkumar, S. (2017). A review on green synthesis of zinc oxide nanoparticles–an eco-friendly approach. *Res.-Eff. Tech.*, **3,** 406-413. DOI:10.1016/j.reffit.2017.03.002

Albalawi, M.A.; Hafez, A.M.; Elhawary, S.S.; Sedky, N.K.; Hassan, O.F.; Bakeer, R.M.; El hadi, S.A.; EL-desoky, A.H.; Mahgoub, S.; Mokhtar, F.A. (2023). The medicinal activity of lyophilized aqueous seed extract of Lepidium sativum L. in an androgenic alopecia model. *Sci. Rep.*, **13**, 7676. DOI:10.1038/s41598-023-33988-1

Al-Saran, N.; Subash-babu, P.; AL-harbi, L.N.; Alrfaei, B.M.; Alshatwi, A.A. (2024). Neuroprotective effect of solid lipid nanoparticles loaded with lepidium sativum (l.) seed bioactive components enhance bioavailability and Wnt/B-Catenin/Camk-Ii Signaling Cascade In Sh-Sy5y neuroblastoma cells. *Nanom.*, **14**, 199. DOI:10.3390/nano14020199

Ann, L.C.; Mahmud, S.; Seeni, A.; Bakhori, S.K.M.; Sirelkhatim, A.; Mohamad, D.; Hasan, H. (2015). Structural morphology and *in vitro* toxicity studies of nano-and micro-sized zinc oxide structures. *J. Env. Chem. Eng.*, **3**, 436-444. DOI:10.1016/j.jece.2014.12.015

Ben Farhat, M.; Mehdaoui, Y.; Selmi, S.; Saidani-tounsi, M.; Abdelly, C. (2024). Domestic cooking effects on nutritional quality and phytochemical contents of zinc biofortified *Lepidium sativum* L. sprouts. *Int. J. Env. Health Res.*, 1-11. DOI:10.1080/09603123.2024.2345376

Bhattacharyya, K.; Kumar, A.; Tyagi, D.; Tripathi, A.; Tyagi, A. (2024). Role of constituent oxides for thermal mineralization of o-dichloro benzene over mixed-oxide-TiO_2 catalysts: A mechanistic explanation. *Chem.*, e202300472. DOI:10.1002/cphc.202300472

Dutra, E.A.; Kedor-hackmann, E.R.M.; Santoro, M.I.R.M. (2004). Determination of sun protection factor (SPF) of sunscreens by ultraviolet spectrophotometry. *Rev. Brasileira de Ciências Farm.*, **40**, 381-385. DOI:10.1590/S1516-93322004000300014

El-Hendawy, A.N.A. (2006). Variation in the FTIR spectra of a biomass under impregnation, carbonization and oxidation conditions. *J. Ana. App. Pyr.*, **75**, 159-166. DOI:10.1016/j.jaap.2005.05.004

Fakhari, S.; Jamzad, M.; Kabiri fard, H. (2019). Green synthesis of zinc oxide nanoparticles: A comparison. *Green chem. lett. rev.*, **12**, 19-24. DOI:10.1080/17518253.2018.1547925

Feng, Y.; Lin, S.; Huang, S.; Shrestha, S.; Conibeer, G. (2015). Can Tauc plot extrapolation be used for direct-band-gap semiconductor nanocrystals? *J. App. Phys.*, **117**, 125701. DOI:10.1063/1.4916090

Georgakopoulos, A. (2003). Study of low rank Greek coals using FTIR spectroscopy. *Energy sources,* **25**, 995-1005. DOI:10.1080/00908310390232442

Gipson, K.; Stevens, K.; Brown, P.; Ballato, J. (2015). Infrared spectroscopic characterization of photoluminescent polymer nanocomposites. *J. Spectr.*, **2015**. DOI:10.1155/2015/489162

Kaur, B. (2023). Physical photoprotection, cosmetic camouflage, and sunscreens. *Ess. Aesth. Derm. Ethnic Skin CRC Press*, 85-99. DOI:10.1201/9780429243769

Khan, M.M.; Saadah, N.H.; Khan, M.E.; Harunsani, M.H.; Tan, A.L.; Cho, M.H. (2019). Potentials of costus woodsonii leaf extract in producing narrow band gap ZnO nanoparticles. *Mat. Sci. Semi. Proc.*, **91**, 194-200. DOI:10.1016/j.mssp.2018.11.030

Mbanga, L.; Mulenga, M.; Mpiana, P.; Bokolo, K.; Mumbwa, M.; Mvingu, K. (2014). Determination of sun protection factor (SPF) of some body creams and lotions marketed in Kinshasa by ultraviolet spectrophotometry. *Inter. J. Adv. Res. Chem. Sci. (IJARCS),* **1**, 7-13.

Mesías, L.G.G.; Qwisgaard, A.M.R.; Untivero, G.P.C.; Kobayashi, L.A.P.; Shimabukuro, L.E.M.; Sugahara, A.A.K. (2017). Comparison of the photoprotective effects of sunscreens using spectrophotometric measurements or the survivability of yeast cells exposed to UV radiation. *Rev. Soc. Quí. Perú,* **83**, 294-307.

Mohamed, M.A.; Jaafar, J.; Ismail, A.; Othman, M.; Rahman, M. (2017). Fourier transform infrared (FTIR) spectroscopy. *Memb. Chara. Elsevier*, 3-29. DOI:10.1016/B978-0-444-63776-5.00001-2

Nkosi, S.B.M.; Thembane, N. (2024). Physical, chemical and biological characteristics of clays from Durban (South Africa) for applications in cosmetics. *Ana. Sci. Adv.,* **5**(3-4), 2300062. DOI:10.1002/ansa.202300062.

Oh, S.Y.; Yoo, D.I.; Shin, Y.; Kim, H.C.; Kim, H.Y.; Chung, Y.S.; Park, W.H.; Youk, J.H. (2005). Crystalline structure analysis of cellulose treated with sodium hydroxide and carbon dioxide by means of X-ray diffraction and FTIR spectroscopy. *Carbo. Res.,* **340**, 2376-2391. DOI:10.1016/j.carres.2005.08.007

Ovais, M.; Khalil, A.T.; Islam, N.U.; Ahmad, I.; Ayaz, M.; Saravanan, M.; Shinwari, Z.K.; Mukherjee, S. (2018). Role of plant phytochemicals and microbial enzymes in biosynthesis of metallic nanoparticles. *App. microb. biotech.*, **102**, 6799-6814. DOI:10.1007/s00253-018-9146-7

Panahi, H.K.S.; Hosseinzadeh-Bandbafha, H.; Dehhaghi, M.; Orooji, Y.; Mahian, O.; Shahbeik, H.; Kiehbadroudinezhad, M.; Kalam, M.A.; Karimi-Maleh, H.; Jouzani, G.S. (2024). Nanotechnology applications in biodiesel processing and production: A comprehensive review. *Renew. Sust. Energy Rev.*, **192**, 114219. DOI:10.1016/j.rser.2023.114219

Pirtarighat, S.; Ghannadnia, M.; Baghshahi, S. (2019). Green synthesis of silver nanoparticles using the plant extract of Salvia spinosa grown *in vitro* and their antibacterial activity assessment. *J. Nanostr. Chem.*, **9**, 1-9. DOI:10.1007/s40097-018-0291-4

Pniewska, A.; Kalinowska-Lis, U. (2024). A survey of UV filters used in sunscreen cosmetics. *App. Sci.*, **14**, 3302. DOI:10.3390/app14083302

Qin, L.; Shing, C.; Sawyer, S.; Dutta, P.S. (2011). Enhanced ultraviolet sensitivity of zinc oxide nanoparticle photoconductors by surface passivation. *Opt. Mat.*, **33**, 359-362. DOI:10.1016/j.optmat.2010.09.020

Sabir, S.; Arshad, M.; Chaudhari, S.K. (2014). Zinc oxide nanoparticles for revolutionizing agriculture: synthesis and applications. *Sci. World J.*, **2014**(1), 925494. DOI:10.1155/2014/925494

Senthilkumar, S.; Sivakumar, T. (2014). Green tea (Camellia sinensis) mediated synthesis of zinc oxide (ZnO) nanoparticles and studies on their antimicrobial activities. *Int. J. Pharm. Pharm. Sci.*, **6**, 461-465.

Shchepkin, A.; Vasilyev, G.; Ostryakov, V.; Pavlov, A. (2024). Sharp rise in cosmic ray irradiation of organisms on earth caused by a nearby sn shockwave passage. *Astrobio.*, **24**(6). DOI:10.1089/ast.2023.0126

Sudhahar, V. (2013). Balasubramanian V. sun production factor (SPF) determination of marketed sunscreen formulation by *in-vitro* method using UV-VIS spectrophotometer. *Arch. App. Sci. Res.*, **5**, 119-122.

Tan, J.; Liu, P.; Gong, P.; Liu, Y.; Chen, J.; Li, R.; Tu, C. (2023). Enhanced self-sintering mechanical strength of carbon blocks via removal of light molecular-weight compound in green petroleum coke. *Fuel*, **343**, 127912. DOI:10.1016/j.fuel.2023.127912

Tariq, M.; Noor, S.; Sarfaraz, S.; Muhammad, S.; Ayub, K. (2023). Flavonoids as selective chemosensor for formic acid over ammonia; a DFT study. *Mat. Today Comm.*, **34**, 105038. DOI:10.1016/j.mtcomm.2022.105038

Thambidurai, S.; Gowthaman, P.; Venkatachalam, M.; Suresh, S. (2020). Natural sunlight assisted photocatalytic degradation of methylene blue by spherical zinc oxide nanoparticles prepared by facile chemical co-precipitation method. *Optik*, **207**, 163865. DOI:10.1016/j.ijleo.2019.163865

Varadavenkatesan, T.; Lyubchik, E.; Pai, S.; Pugazhendhi, A.; Vinayagam, R.; Selvaraj, R. (2019). Photocatalytic degradation of Rhodamine B by zinc oxide nanoparticles synthesized using the leaf extract of *Cyanometra ramiflora*. *J. Photoch. Photob. B: Bio.*, **111621**. DOI:10.1016/j.jphotobiol.2019.111621

Vijayalakshmi, R.; Rajendran, V. (2012). Synthesis and characterization of nano-TiO_2 via different methods. *Arch. App. Sci. Res.*, **4**, 1183-1190.

Vijayaram, S.; Razafindralambo, H.; Sun, Y.Z.; Vasantharaj, S.; Ghafarifarsani, H.; Hoseinifar, S. H.; Raeeszadeh, M. (2024). Applications of green synthesized metal nanoparticles-a review. *Bio. Trace Ele. Res.*, **202,** 360-386. DOI:10.1007/s12011-023-03645-9

Xie, C.; Wilson, B.A.; Qin, Z. (2024). Regulating nanoscale directional heat transfer with Janus nanoparticles. *Nanos. Adv*. **6**, 3082-3092. DOI:10.1039/D3NA00781B

تأثير المركبات الخضراء جسيمات أكسيد الزنك النانوية على عامل الحماية من الشمس في كريم الحماية من حروق الشمس

هيمداد حمد عزيز

قسم الفيزياء/ كلية التربية/ شقلاوة/ جامعة صلاح الدين–أربيل/ العراق

بيستون أنور كوزة

قسم تكنولوجيا المعلومات/ كلية شقلاوة التقنية/ جامعة أربيل التقنية/ العراق

هيرو حمد عزيز

مركز أربيل التعليمي للأمراض الجلدية/ العراق

لارى حنا صليوة

قسم الفيزياء/ كلية العلوم/ جامعة صلاح الدين–أربيل/ العراق.

الملخص

في العصر الحديث، هناك تركيز كبير على التخليق الأخضر، الذي يتضمن إنتاج الجسيمات النانوية بطريقة صديقة للبيئة دون استخدام المواد الكيميائية الضارة أو المذيبات السامة. هذا النهج، الذي يحظى بشعبية خاصة في الطرق البيولوجية، قد لفت انتباها كبيراً. استغلال المصادر الطبيعية مثل النباتات والكائنات الدقيقة هو أسلوب شائع للتخليق الأخضر. بين أكاسيد المعادن، تعتبر جسيمات أكسيد الزنك النانوية الثانية الأكثر انتشارًا بسبب تكلفتها الفعالة وسلامتها وسهولة تحضيرها. تم تخليق جسيمات أكسيد الزنك باستخدام نهج مستدام يشمل استخراج نبات (Lepidium sativum L.) وzinc acetate dihydrate. خضعت جسيمات أكسيد الزنك النانوية لتقنيات توصيف شاملة لتحليل هيكلها وتشكيل سطحها وخصائصها البصرية والكيميائية. أظهرت جسيمات أكسيد الزنك حجماً بلورياً متوسطاً يبلغ 26.78 نانومترًا، مع تأكيد FE-SEM لحجم جسيم النانو المتكتل المتوسط بلغ 64 نانومترًا. بعد ذلك، تم دمج نسب متفاوتة من هذه الجسيمات النانوية في مستحضر كريم حماية من حروق الشمس لدراسة تأثيرها على تعزيز عامل حماية من الشمس (SPF) للمستحضر. أظهرت النتائج زيادة ملحوظة في عامل حماية من الشمس مع تركيزات ZnO NPs الأعلى.

الكلمات الدالة: أكسيد الزنك، عامل حماية من الشمس، حيود الأشعة السينية، التحليل الطيفي بالأشعة السينية المشتتة للطاقة والتوليف الأخضر.